17th World Conference on Earthquake Engineering, 17WCEE
Sendai, Japan - September 13th to 18th 2020

A COMPARISON OF STRUCTURAL AND FOUNDATION ROCKING USING A MODIFIED NONLINEAR-WINKLER-FOUNDATION MODEL

I. Pelekis[(1)], F. McKenna[(2)], G. Madabhushi[(3)], M. DeJong[(4)]

[(1)] *PhD Candidate, University of Cambridge, UK, ip312@cam.ac.uk*
[(2)] *Research Engineer, University of California, Berkeley, USA, fmckenna@berkeley.edu*
[(3)] *Professor, University of Cambridge, UK, mspg1@cam.ac.uk*
[(4)] *Assistant Professor, University of California, Berkeley, USA, dejong@berkeley.edu*

Abstract

Seismic isolation by means of rocking action is an effective way to reduce the damage demand on a building during ground excitation. The rocking response largely depends on the energy dissipation resulting from soil-structure interaction, but also on the impact loading that occurs during re-centering. This paper deals with the computational modelling of buildings that have pad footings on dry sand and are allowed to respond with structural or foundation rocking. A Beam-on-Nonlinear-Winkler-Foundation (BNWF) model from the OpenSees environment serves as a base for a newly modified model (termed mBNWF) that allows a more realistic response of uplifting footings on soil. First, the mBNWF involves an uplift-dependent stiffness and viscosity transmission for vertical and horizontal directions, along with a friction to vertical force coupling. Secondly, the phenomenon of complete separation of the footing from the soil is captured through friction-gap elements in OpenSees. This modelling approach is used to simulate the response of a building that can uplift and rotate at the column/footing interface allowing structural "rocking above" the foundations (termed RA), and a building with similar dynamic characteristics but that has fixed footing-to-column connections allowing "rocking below" the foundations (termed RB). The model requires a relatively small number of soil and structural parameters as input, which can be determined directly from experimental data, or from the literature. After validation of the mBNWF model using centrifuge test data for a variety of ground excitations and for different types of sand, a computational comparison between structural and foundation rocking is carried out using incremental dynamic analysis (IDA). Earthquake records with characteristics that are specifically damaging for rocking systems (for instance, records with long duration pulses or large velocity pulses) are selected from the PEER database for a multi-record IDA. IDA results indicate that PGV provides a reasonably good IM to predict both rocking angle and storey drift, and that both structural and foundation rocking effectively isolate the structures by capping storey drifts. Additionally, the RA structure had higher variability in the response, likely due to stronger impacts at re-centering, and loose sand reduced both storey drifts and rocking rotations compared to dense sand. Overall, the validated mBNWF model allowed a more detailed and extensive comparison of structural versus foundation rocking than was feasibly possible through experimental centrifuge testing.

Keywords: Rocking, Winkler Foundation, Soil-Structure Interaction, OpenSees, Incremental Dynamic Analysis

1. Introduction

Designing for structural or foundation rocking response of structural systems during earthquake excitations can be an effective approach to reduce damage. The recognition of the beneficial effects of structural [1,2] and foundation [3,4] rocking has generated the need for computational models that can accurately describe the rocking response, including effects from soil-foundation and foundation-superstructure interactions. Such models can further be used within a wider assessment scheme that explores the relative differences between structural and foundation rocking.

A common model that describes the soil-foundation interaction is the Beam-on-nonlinear Winkler Foundation (BNWF) spring model [5]. This model is attractive due to the relative low number of input parameters required which can, in addition, be directly linked to soil properties. However, some limitations arise as a result of the simplistic, spring nature of the model as opposed to other families of complicated models [6,7]. Limitations include the lack of soil dilation effects or laterally constraining the foundation in total loss of contact with the soil.

This paper presents a modified version of the currently available in OpenSees BNWF model (mBNWF) and uses that model to investigate the performance of rocking systems. mBNWF model predictions of the earthquake response of buildings with structural and foundation rocking were validated against a series of centrifuge tests. Specifically, the centrifuge campaign involved two nearly dynamically equivalent buildings with structural and foundation rocking being subjected to sequential earthquake excitations on dry sand. For structural rocking, one building model was designed with a column-footing partial hinge for rocking above its foundation level (hereafter named building model RA), and for foundation rocking, another building model was designed with a fixed column-footing connection for rocking below its foundation level (hereafter named building model RB). Taking advantage of the computational models to provide reasonable predictions when compared to the centrifuge obtained response, IDA was employed to further study the response of these systems.

2. Incremental dynamic analysis in the context of rocking

Incremental dynamic analysis (IDA) captures the evolution of seismic behaviour across a range of scales of an earthquake excitation [8]. Using a suite of earthquake excitations, it can provide insights about the variability of the dynamic response of a structure. Typically, an intensity measure (IM) of a specific record, for instance PGA, is a proxy for the seismic demand, and is related to a characteristic engineering demand parameter (EDP) which results from the earthquake response (for instance, story drift ratio).

For building models with a single mass supported on a shallow footing [9], or a caisson foundation [10], use of IDA has shown that allowing rocking results in reduced drifts and a smaller likelihood of collapse compared to equivalent hinging systems. Owing to the re-centering nature of foundation rocking, residual deformations can also be reduced. For instance, for multi-storey buildings with raft foundations rocking on soil, a factor of safety for vertical loading close to 2.5, IDA has shown that residual rotations beyond 2% are unlikely to occur [11]. However, the variability of a foundation rocking system's response can increase as larger deformation demand (settlement, rotation) is placed on the foundation [12].

For rocking of flexible structures on a rigid base there is limited research on the response variability obtained by IDA. For conventional steel braced frames rocking on a rigid base, using $S_a(T_1)$ as IM of far-field records in IDA may not be appropriate, as it can be observed that reducing the number of stories results to a larger dispersion of the IM for a given peak rocking angle (see Fig. 6 in [13]). For flexible structures rocking on rigid base subjected to pulse-like records, it has been shown that shape characteristics of velocity pulses (amplitude, frequency) hidden in earthquake excitations should be considered to obtain an improved estimation of the maximum rocking angle [14]. This follows evidence that the peak ground velocity (PGV) is a good indicator of the maximum rocking angle of rigid rocking bodies [15–17]. However, owing to the multi-modal nature of flexible structures, assessing simultaneously the demand of story drift ratios and rocking angle is necessary in order to compare performance and response variability against other structural systems.

Therefore, in this paper IDA is employed to investigate the difference in variability of the demand in story drift ratio and rocking angle of buildings with structural and foundation rocking founded on dry sand.

3. Modelling of structural and foundation rocking buildings

3.1 Centrifuge testing

Centrifuge testing of two nearly identical buildings with pad foundations on dry sand (Fig. 1a-c) was carried out in a side-by-side configuration, to compare structural and foundation rocking (Fig. 1d), and inform the parameters of the computational modelling. The building models were subjected to sequential earthquake excitations and tested in an artificial gravitational environment at 33g. To enable structural rocking, the columns of the one building model were allowed to step on the footings and thus rocking could develop above the foundation level (hereafter building model referred to as RA). For foundation rocking, the columns of the other building model were clamped to the footings, thus rocking below the foundation level could develop (hereafter building model referred to as RB). In prototype scale, the two models represent 3-4 storey buildings with shallow foundations resting on a sandbed of 7.5m and were designed to remain elastic. A set of excitations, first for a relatively high density (dense sand, D_r = 96%), and then for a relatively medium density (loose sand, D_r = 58%) were used, including pulse-like, cyclic and historic records. Table 1 summarizes the properties of the models and more on the experimental scheme can be found elsewhere [18,19].

3.2 Finite element modelling

The building models and the soil were modelled in OpenSees with the total mass and stiffness represented in a 2D plane. The earthquake response of each building type was modelled separately. The initial conditions were specified as zero rotations and settlements, and prior to the dynamic analysis, a nonlinear static analysis was carried out considering only the self-weight of the buildings. For the superstructure, linear elastic beam/column elements were used which were finely discretized to capture wave propagation from impacts (Fig. 2a, b).

3.2.1 Modelling of foundation-superstructure interface for structural rocking

The footings of model RA contain slots which allow column uplift and provide a pivot point for rotation. To model this interface, the friction-gap element *flatSliderBearing* available in OpenSees (developed by A. Schellenberg) was used. In its default configuration, the element represents a bearing with a flat surface for sliding with friction and allows for zero force transmission in all directions when uplift occurs. In this case, each RA footing had a pair of these elements in an inclined position, a configuration identical to the actual shape of the footing slot (Fig. 2c). The order of magnitude of the element required sliding and axial stiffnesses was estimated by iteratively increasing the stiffness values until the response was no longer affected. In addition, a coefficient of friction of μ = 0.43 was specified. Overall, this approach facilitates the local re-centering capability of the column ends in the RA footing slots, just as it would develop physically.

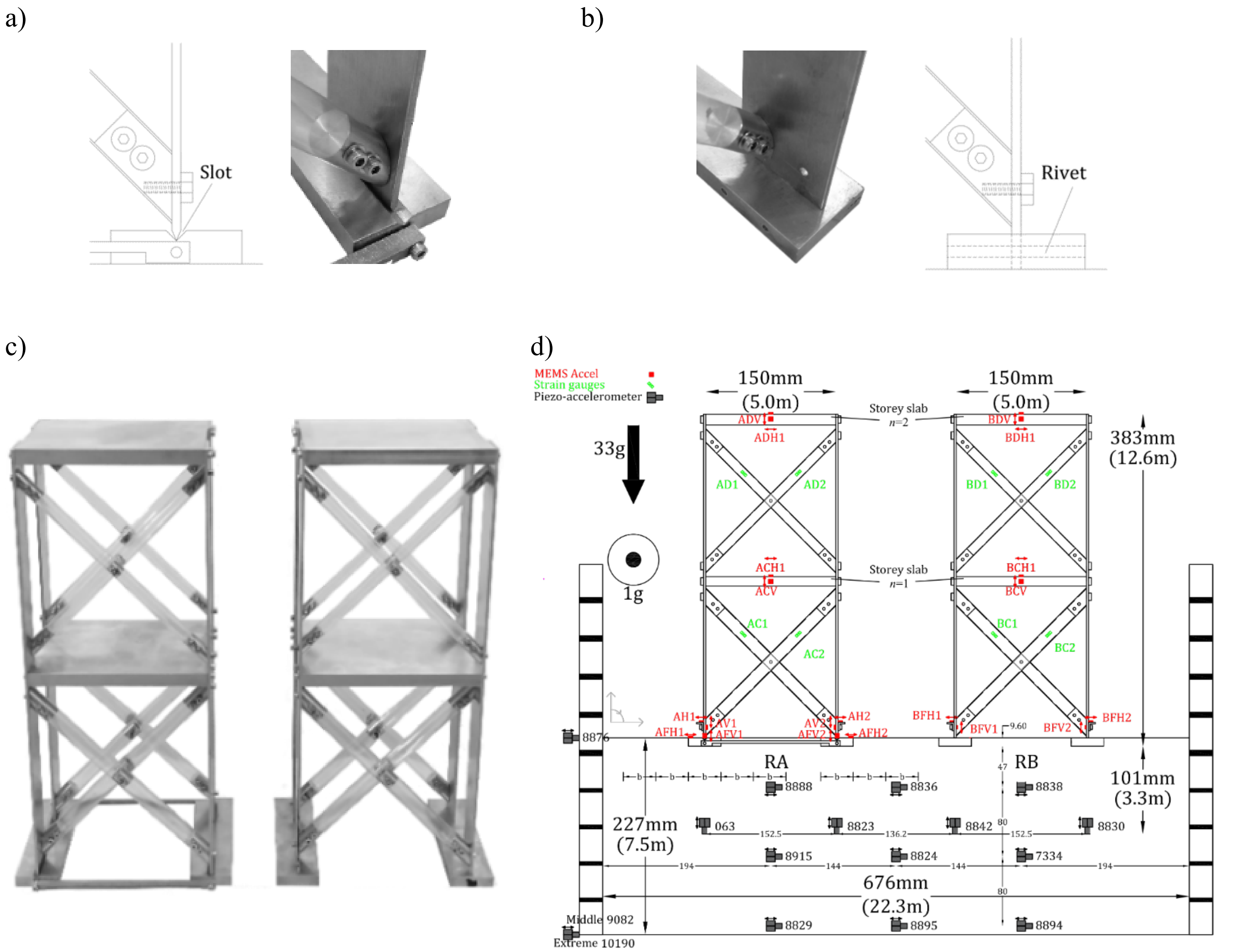

Fig. 1 – RA: Connection for partially hinged support and structural rocking (a), RB: Connection for fixed support and foundation rocking (b), RA model (left) and RB model (right) (c) and cross-sectional view of the centrifuge model with sensor locations and overall dimensions (d).

Table 1 – Characteristics of models RA and RB

Properties	RB		RA	
	Model scale	Prototype scale	Model scale	Prototype scale
1st mode design period	0.019 s	0.66 s	0.020 s	0.70 s
Experimental 1st mode frequency	53 Hz	1.6 Hz	50 Hz	1.5 Hz
Experimental 2nd mode frequency	147 Hz	4.5 Hz	136 Hz	4.1 Hz
Numerical 1st mode frequency	53 Hz	1.6 Hz	50 Hz	1.5 Hz
Numerical 2nd mode frequency	152 Hz	4.6 Hz	141 Hz	4.3 Hz
Total mass of uplifting parts	2.4 kg	86 metric tonnes	2.1kg	75 metric tonnes
*Structural damping ζ_1, ζ_2 for 1st & 2nd mode	$\zeta_1 = 0.0209$, $\zeta_2 = 0.009$		$\zeta_1 = 0.0053$, $\zeta_2 = 0.0066$	
Soil friction angle φ' [20]	33°			
Footing dimensions	37.5 mm x 160 mm x 9.6 mm (1.24 m x 5.28 m x 0.32 m)			
Factor of safety for vertical loading	FoS = 2.3 (80kPa static bearing pressure), Design Approach 1/2, EC7 [21]			
Storey lumped mass ($m_n, n = 1,2$)	m_n=0.83 kg (m_n=30 metric tonnes, prototype scale)			

*Measured in fixed-base conditions from free vibration traces.

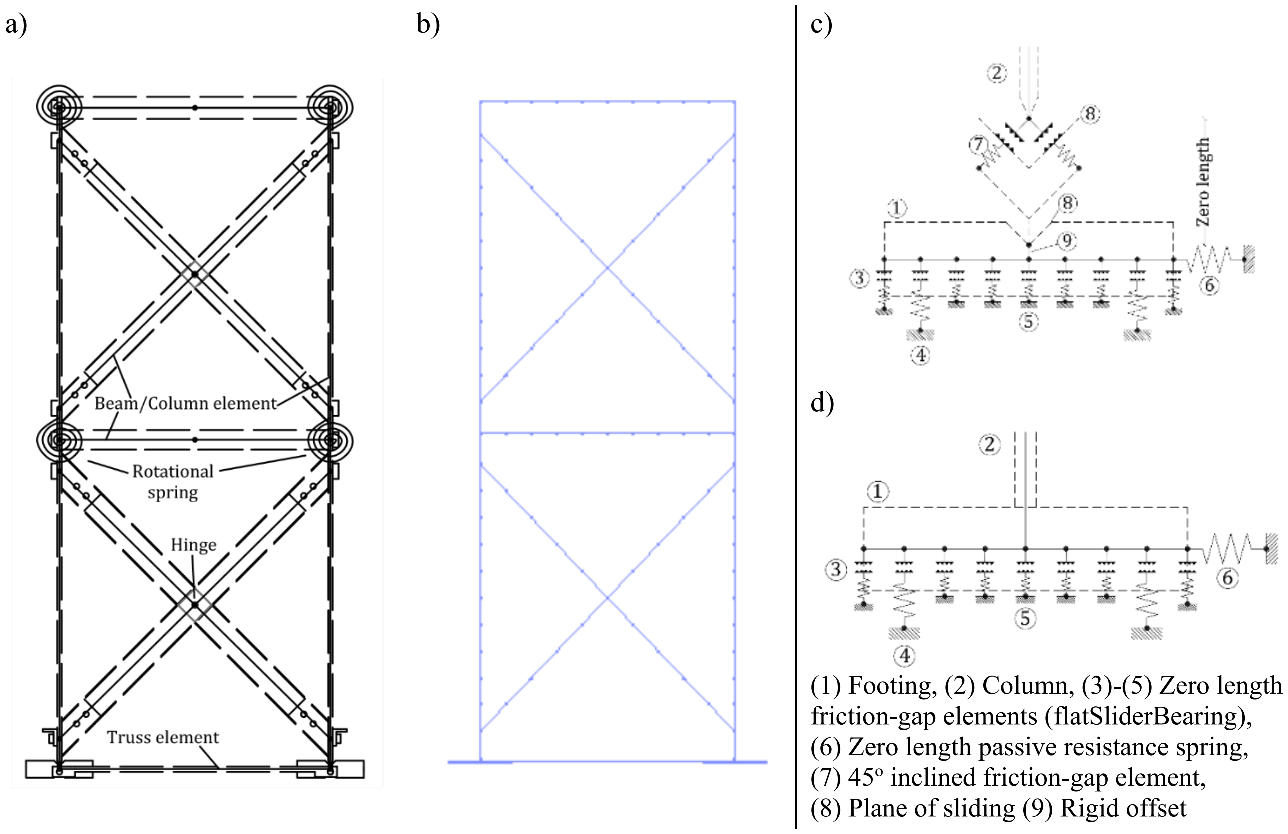

Fig. 2 – Basic element discretization (a) and refined configuration (b) for model RA and soil-footing-column detail for model RA (c) and model RB (d)

3.2.2 Modelling of soil-foundation interface for foundation rocking

A modified version of the BNWF model was used to account for soil-foundation interaction for dry sand (hereafter referred to as mBNWF). The BNWF model comprises of a series of vertical springs that are distributed below a rigid footing. This enables the caption of vertical and rotational resistance of the soil. To account for sliding on the soil and passive resistance, two lateral springs are attached at the footing's end. The constitutive law of the vertical springs allows for gapping, inelastic response for large settlement increments and linear elastic response for small settlement increments. The parameters controlling the constitutive law were calibrated against a series of centrifuge experiments, and the model has been found to replicate well the rocking of single footings, including moment-rotation response and energy dissipation capability [5].

One of the main limitations of the BNWF model is that total loss of contact of the footing with the soil cannot be replicated accurately. This limitation stems from the independency between the vertical springs that incorporate the gapping capability and the lateral springs which do not. Specifically, the spring for sliding constrains fully the footing in the lateral direction and upon partial or no contact no reduction of the frictional force is specified. To overcome this problem, the lateral spring for sliding can be removed, and instead each vertical spring can be replaced with a friction-gap *flatSliderBearing* element that maintains the constitutive law in the vertical direction. First, this change allows locally for an uplift based transmission of forces in both vertical and horizontal directions. Secondly, there is local coupling between the frictional and vertical forces, which can be governed by the friction angle of the sand.

An example of the performance of two soil-foundation models is shown in Fig. 3 (see Table 2 for input used). This example is from a cyclic excitation with large amplitude with a frequency close to the natural frequency of the building models in centrifuge testing. When the BNWF model is employed for the

RB footings, a non-zero lateral force is maintained at the point of zero vertical force (see RB footings, Fig. 3a). On the contrary, when the mBNWF model is employed, all forces reach zero simultaneously (see RB footings, Fig. 3b). The error in terms of lateral displacements can be significant, not only between the two computational responses (Fig. 4a, b), but also between the numerical and the experimental responses (Fig. 4a). If the response is high-pass filtered at 10 Hz (model scale frequency), the residual displacements can be removed, and be compared directly to the displacements derived from the experimental tests. Fig. 4b shows that the mBNWF model (after high-pass filtering) can better capture the response. In addition, a realistic value of lateral residual displacement is obtained.

a) b)

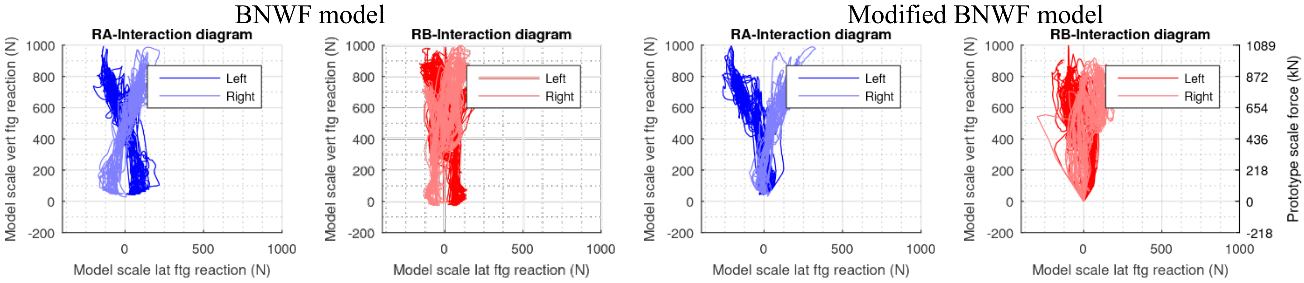

Fig. 3 – Interaction diagrams for the total forces below the left and right footings below RA in loose sand when the BNWF model (a) and the mBNWF model (b) are used

a) b)

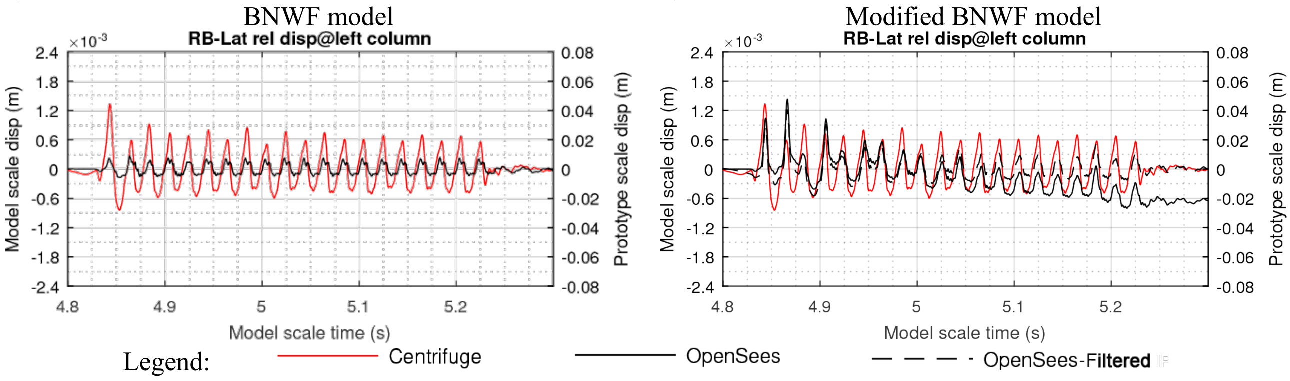

Fig. 4 – Lateral relative displacement of the end node of the left column for model RB

Table 2 – Properties of the mBNWF model and their input values

a) Soil properties

	Dense sand	Loose sand
	Default value	
Cohesion c (kPa)	0.0	
Friction angle φ’ (°)	33.0 [20]	
Soil unit weight γ (kN/m³)	16.3	15.0
Shear modulus G_0 (MPa)	30.0	22.0
Poisson’s ratio ν	0.375	
Damping coeff. and ratio, $c_{x,i}$ (Ns/m) and ζ_x	1.75×10^6 , 0.22	1.44×10^6 , 0.21
Damping coeff. and ratio, $c_{y,i}$ (Ns/m) and ζ_y	2.78×10^6 , 0.63	2.29×10^6 , 0.61
Tensile strength T_p (kPa)	0.0	

b) Soil mesh properties

End length ratio R_e	0.15
Stiffness intensity ratio R_k	6
Spring spacing l_e/l	0.02

Therefore, for the IDA scheme presented next, the mBNWF model was selected. A more comprehensive validation of the wider computational model incorporating the mBNWF against the centrifuge testing of models RA and RB can be found elsewhere [22].

4. Incremental dynamic analysis

Based on the successful simulation of centrifuge testing [22], the mBNWF model is used in this paper to investigate rocking more broadly. Specifically, the IDA results discussed here form a preliminary base for a wider assessment of the performance comparisons between structural and foundation rocking. PGA, PGV and PGD were selected as IMs and were evaluated against the EDPs of peak rocking angle and story drift ratios, for the RA and RB models. This analysis involved a suite of 49 records, scaled independently in 9 increments; after scaling a range of PGV up to approximately 330 cm/s was achieved. The suite consists of the three subgroups, namely far-field records and near field records with and without pulses [23]. Since the superstructure is linear elastic, any nonlinearity would arise from uplift and inelastic response of the soil.

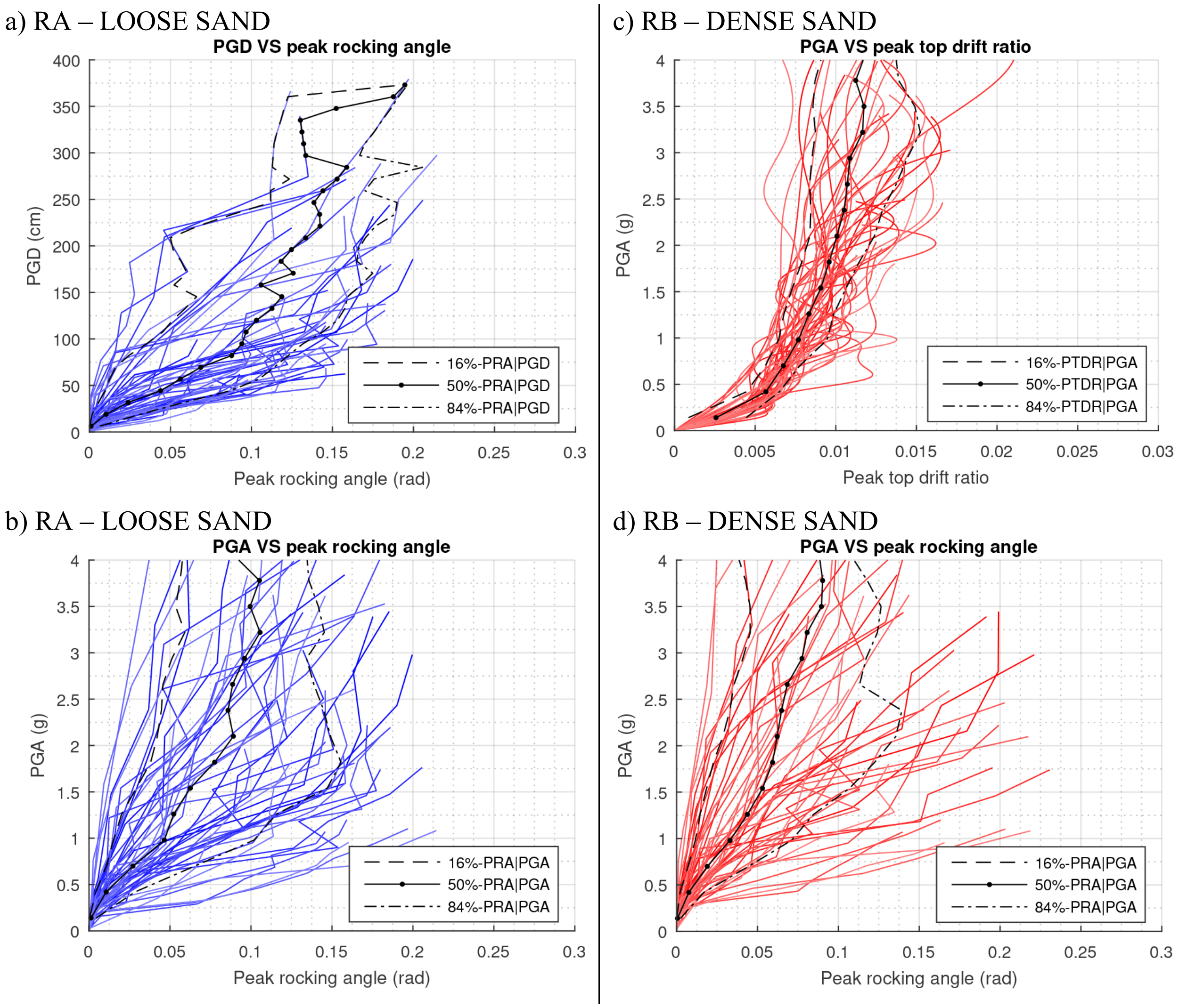

Fig. 5 – Examples of various pairs of IMs and EDMs for model RA in loose sand (a, b) and similarly for model RB in loose sand (c, d)

DENSE SAND

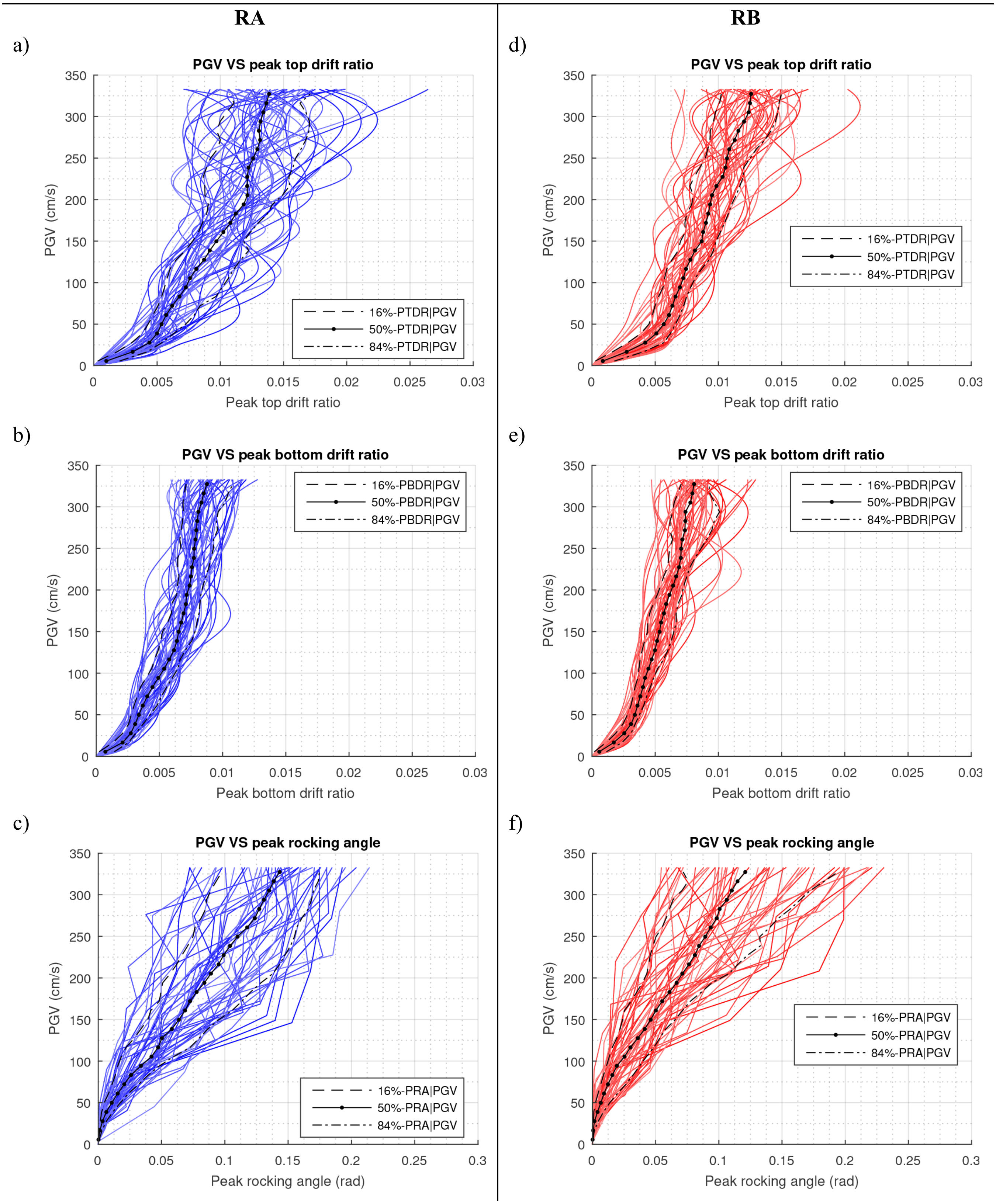

Fig. 6 – Incremental dynamic analyses with PGV as IM and peak top and bottom story drift ratios, and rocking angle for model RA (a-c) and similarly for model RB (d-f) on dense sand.

LOOSE SAND

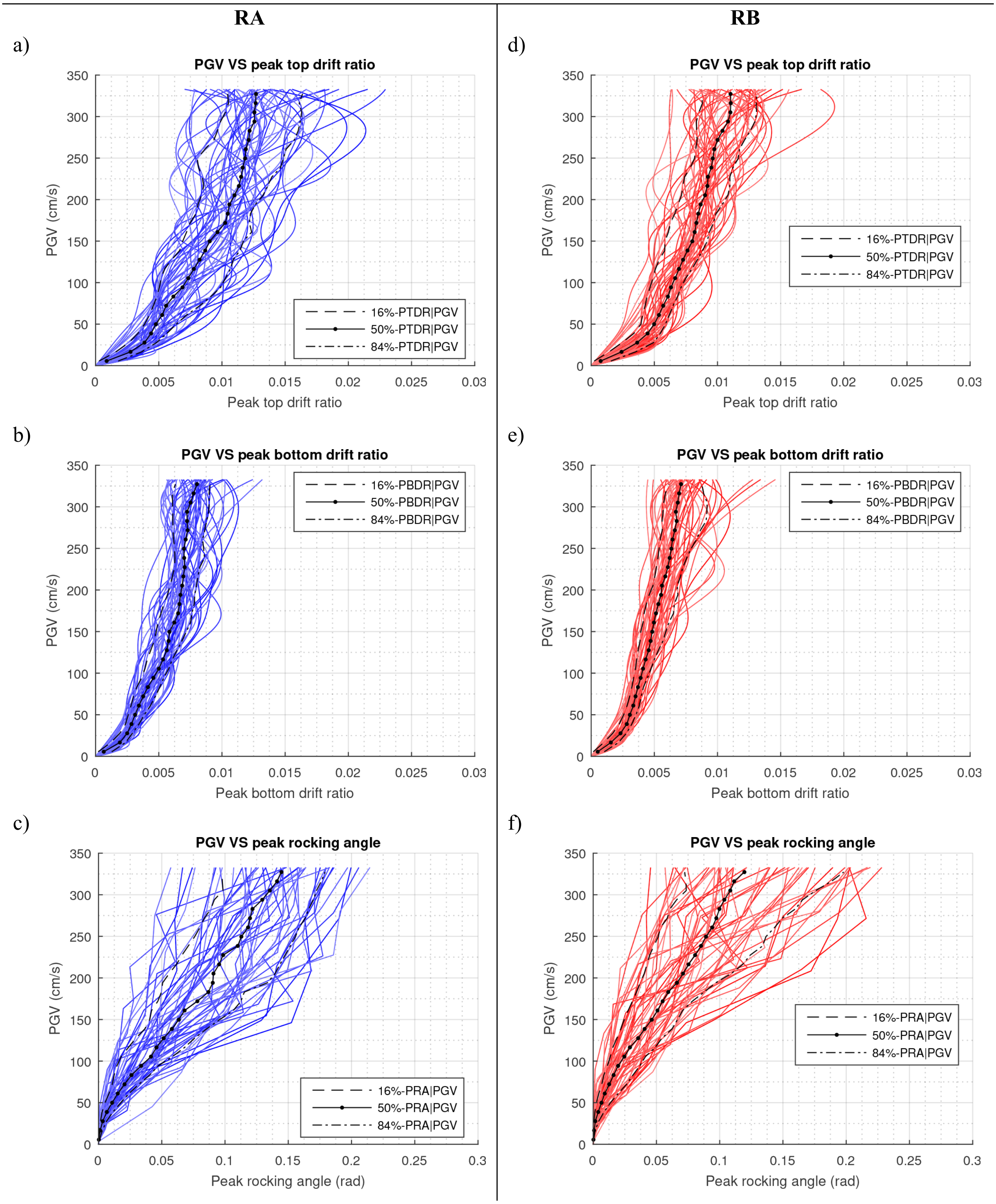

Fig. 7 – Incremental dynamic analyses with PGV as IM and peak top and bottom story drift ratios, and rocking angle for model RA (a-c) and similarly for model RB (d-f) on loose sand.

In general, rocking angles close to the slenderness angle of the building (approximately 0.3 rad) were achieved for some records. However, for the design of rocking structures, an acceptable rocking amplitude would be much smaller than the slenderness angle. Therefore, the range of demand presented here is considered extremely large for practical applications and is only to reveal the mechanisms between structural flexibility, uplift and soil.

PGA is a common IM but is known to be a poor predictor of the rocking amplitude for typical rocking systems such rigid blocks on a rigid base. Comparison of Fig. 5b, d with Fig. 7c and Fig. 6f, respectively, confirms that PGA was a poor indicator for predicting the peak rocking angle of both models RA and RB, while PGV provides considerably smaller dispersion. PGD also appears to provide a very large dispersion (Fig. 5a). For peak top storey drift ratio, PGA provides a reasonably good prediction, but again the PGV provided a better prediction (Fig. 5c and Fig. 6d).

Overall, Figs. 6 and 7 indicate that PGV can be a good predictor of peak story drift ratios and rocking angles for both models RA and RB, across both dense and loose sand.

More specifically, Figs. 6 and 7 indicate that PGV is well correlated with both the bottom storey drift ratio and the rocking angle, with this trend being stronger for model RB. The fact that the EDPs for RA and RB are similarly correlated to the PGV confirms that rocking behavior is effectively capping the drift demands in both cases. However, the variability in response is noticeably smaller for model RB. Additionally, the cap is smaller for the loose sand case and model RB, suggesting that larger deformations on the soil can allows for a reduced baseline of demand in the superstructure.

The top storey drifts show a larger dispersion when compared to the bottom story counterparts for both buildings in all density cases. This suggests that a higher mode of response is triggered either due to the rotational motion of the buildings or because of the impacts generated during re-centering. This dispersion is larger for model RA when compared to RB. A reason for this might be that less energy is dissipated when an RA column lands back to its footings or that upon uplift significantly less damping is provided to the rotational motion of the building as opposed to RB, for which the soil can provide damping when the footing rotates, and thus when the whole building rotates. Further investigation with more EDPs obtained from the footings' response is ongoing.

5. Conclusion

Seismic protection of structures with rocking isolation is a promising approach in reducing the damage demand placed in the superstructure during earthquakes. This paper addresses the modelling and response of buildings with structural and foundation rocking in order to better understand the behavior of these systems. An improved version of the common Beam on Nonlinear Winkler Foundation model to account for realistic response of footings experiencing partial or total loss of contact is briefly presented. This soil-footing model forms part of larger computational models that intend to capture the interaction between rocking and structural flexibility, in conjunction with the soil-structure interaction.

Taking advantage of this integrated modelling approach, incremental dynamic analysis was performed for flexible buildings with pad footings on dry sand representing structural and foundation rocking. Preliminary results indicate that peak ground velocity is an appropriate intensity measure to describe both the demand due to flexural vibrations while rocking and the rocking amplitude. A larger dispersion in the engineering demand parameters was observed for structural rocking, since this utilizes soil at a lesser degree than foundation rocking, thus resulting in smaller damping of flexural vibrations and rocking. A more thorough analysis incorporating engineering demand parameters of the foundation would be necessary to reveal any interacting mechanisms to a greater extent.

6. References

[1] Housner GW. The behaviour of inverted pendulum structures during earthquakes. *Bulletin of Seismological Society of America* 1963; **53**(2): 403–417.

[2] Makris N. A half-century of rocking isolation. *Earthquakes and Structures* 2014; **7**(6): 1187–1221.

[3] Taylor PW, Barlett PE, Wiessing PR. Foundation Rocking under Earthquake Loading. *Le Mouvement Des Semelles Dans Les Tremblements de Terre* 1980: 313–322.

[4] Gazetas G. 4th Ishihara lecture: Soil-foundation-structure systems beyond conventional seismic failure thresholds. *Soil Dynamics and Earthquake Engineering* 2015; **68**: 23–39.

[5] Raychowdhury P, Hutchinson TC. Performance evaluation of a nonlinear Winkler-based shallow foundation model using centrifuge test results. *Earthquake Engineering and Structural Dynamics* 2009; **38**: 679–698.

[6] Lu Y, Wang Z. Characterization of structural effects from above-ground explosion using coupled numerical simulation. *Computers and Structures* 2006; **84**: 1729–1742.

[7] Heron CM, Haigh SK, Madabhushi SPG. A new macro-element model encapsulating the dynamic moment–rotation behaviour of raft foundations. *Géotechnique* 2015; **65**(5): 442–451.

[8] Vamvatsikos D, Cornell CA. Incremental dynamic analysis. *Earthquake Engineering and Structural Dynamics* 2002; **514**: 491–514.

[9] Deng L, Kutter BL, Kunnath SK. Probabilistic Seismic Performance of Rocking-Foundation and Hinging-Column Bridges. *Earthquake Spectra* 2012; **28**(4): 1423–1446.

[10] Zafeirakos A, Gerolymos N, Drosos V. Incremental dynamic analysis of caisson – pier interaction. *Soil Dynamics and Earthquake Engineering* 2013; **48**: 71–88. DOI: 10.1016/j.soildyn.2013.01.021.

[11] Masaeli H, Khoshnoudian F, Musician S. Incremental dynamic analysis of nonlinear rocking soil-structure systems. *Soil Dynamics and Earthquake Engineering* 2018; **104**: 236–249. DOI: 10.1016/j.soildyn.2017.09.013.

[12] Pecker A, Chatzigogos CT. Non linear soil structure interaction : impact on the seismic response ostructures. *XIV European Conference on Earthquake Engineering, August 2010, Ohrid, FYROM*, 2010. DOI: 10.1007/978-90-481-9544-2.

[13] Vetr MG, Nouri AR, Kalantari A. Seismic evaluation of rocking structures through performance assessment and fragility analysis. *Earthquake Engineering and Engineering Vibration* 2016; **15**(1): 115–127.

[14] Acikgoz S, DeJong MJ. The interaction of elasticity and rocking in flexible structures allowed to uplift. *Earthquake Engineering & Structural Dynamics* 2012; **41**(11): 2177–2194.

[15] Kavvadias IE, Papachatzakis GA, Bantilas KE, Vasiliadis LK, Elenas A. Rocking spectrum intensity measures for seismic assessment of rocking rigid blocks. *Soil Dynamics and Earthquake Engineering* 2017; **101**: 116–124.

[16] Kavvadias IE, Vasiliadis LK, Elenas A. Seismic Response Parametric Study of Ancient Rocking Columns. *International Journal of Architectural Heritage* 2017; **11**(6): 791–804.

[17] Giouvanidis AI, Dimitrakopoulos EG. Rocking amplification and strong-motion duration. *Earthquake Engineering & Structural Dynamics* 2018; **47**: 2094–2116.

[18] Pelekis I, Madabhushi SPG, DeJong MJ. Seismic performance of buildings with structural and foundation rocking in centrifuge testing. *Earthquake Engineering and Structural Dynamics* 2018; **47**(12): 2390–2409.

[19] Pelekis I, Madabhushi GSP, DeJong MJ. Soil behaviour beneath buildings with structural and foundation rocking. *Soil Dynamics and Earthquake Engineering* 2018; **123**: 48–63.

[20] Shepley P. Water injection to assist pile jacking. University of Cambridge. PhD Thesis, 2013.

[21] CEN. Eurocode 7: Geotechnical design - Part 1: General rules 2004.

[22] Pelekis I, McKenna F, Madabhushi GSP, DeJong MJ. Finite element modelling of buildings with structural and foundation rocking on dry sand. *Earthquake Engineering and Structural Dynamics (in Review)*.

[23] Gavin H. Summary of the ATC-63 Strong Ground Motion Data Sets. http://people.duke.edu/~hpgavin/cee541/ATC63-readme.html.